September 25th - 28th, 2017
NTERFACES
architecture . engineering . science IASS 2017 hamburg

Proceedings of the IASS Annual Symposium 2017
"Interfaces: architecture.engineering.science"
25 - 28th September, 2017, Hamburg, Germany
Annette Bögle, Manfred Grohmann (eds.)

Force density method for simultaneous optimization of geometry and topology of spatial trusses

Kazuki Hayashi*, Makoto Ohsaki[a], Caitlin Mueller[b]

*Dept. of Architecture and Architectural Engineering, Graduate School of Engineering, Kyoto University
Kyoto-Daigaku Katsura, Nishikyo, Kyoto, 615-8540, Japan
hayashi.kazuki.55a@st.kyoto-u.ac.jp

[a] Dept. of Architecture and Architectural Engineering, Graduate School of Engineering, Kyoto University
[b] Building Technology Program, School of Architecture + Planning, Massachusetts Institute of Technology

Abstract

Force density method is applied to simultaneous optimization of geometry and topology of truss structures. Compliance under single loading condition is minimized for specified structural volume. Force density is the ratio of axial force to the member length. The difficulties due to existence of melting nodes, closely spaced nodes connected by extremely short members, are successfully avoided by considering force density as design variable, so that various optimal shapes can be otained from a sparse initial ground structure. By using the fact that the optimal truss is statically determinate with the same absolute value of stress in existing members, the compliance and the structural volume are expressed as explicit functions of force density only, and optimal solutions are found with small computational cost. The formulation process of the optimization problems is described, then accuracy, efficiency, and applicability of the proposed method are demonstrated through three numerical examples; a plane truss model is optimized first, and spatial structures are discussed next.

Keywords: Truss, Simultaneous optimization of topology and geometry, Force density method, Compliance

1. Introduction

Various methods of mathematical programming and heuristic approaches have been developed for topology optimization (Bendsøe and Sigmund [1], Ohsaki [2]). The ground structure method (Dorn *et al.* [3]) is the most frequently used approach among them; however, it requires enormous computational cost to obtain a sparse optimal truss with appropriate nodal locations, because a densely connected initial ground structure with many nodes should be used to optimize the geometry and topology.

In optimizing the geometry of a truss, not only nodal coordinates but also cross-sectional areas are often chosen as design variables, and the thin members after optimization are to be eliminated. This way, we can optimize the truss geometry and topology simultaneously. However, if the nodes are allowed to move in a wide range of the design space, closely spaced nodes connected by extremely short members will exist (Ohsaki [2], Achtziger [4]) . These nodes are called "melting nodes", which trigger numerical problems; i.e., axial stiffness and the sensitivity coefficients of stiffness of a short member have very large values.

Some methods have been proposed to overcome the difficulties related to melting nodes. A growth method (McKeown [5], Hagisita and Ohsaki [6]) starts with a simple truss and adds nodes and members successively by heuristics. This method leads to an optimal truss with sparse topology and geometry; however, it does not satisfy any theoretical optimality criteria. Achtziger [4] reformulated the optimization problem by setting nodal displacements in addition to nodal coordinates and cross-sectional areas as design variables. However, the constraint to avoid melting nodes is still necessary.

In this paper, force density method is applied to the formulation on simultaneous optimization of geometry and topology of truss structures (Ohsaki and Hayashi [7]). Force density method has been used mainly for form-finding of cable nets and tensegrity structures (Schek [8], Zhang and Ohsaki [9]). The difficulties due to melting nodes are successfully avoided by considering force density as design variable, which enables us to obtain various optimal shapes from a sparse initial ground structure. Moreover, this method can reduce computational cost, because the number of variables is equal to that of members. However, the optimization process sometimes diverges, and the optimal solution strongly depends on the initial solution.

This paper focuses on improvement of the formulation based on this force density method to optimize the geometry and topology of trusses simultaneously with small computational cost. Three numerical examples are presented to evaluate accuracy, efficiency, and applicability of this method.

2. Force density method

In this section, force density method is explained for application to truss topology optimization (Ohsaki and Hayashi [7]). Free nodal coordinates and reaction forces at fixed nodes are expressed as functions of force density, which is the ratio of axial force to length. Force density q_i of member i is defined with respect to the axial force N_i and length L_i as

$$q_i = \frac{N_i}{L_i} \tag{1}$$

Consider a truss with n nodes and m members. If member i connects nodes j and k, then the components of connectivity matrix $\mathbf{C} \in \mathbb{R}^{m\times n}$ are defined as

$$C_{ij} = -1, \quad C_{ik} = 1 \quad (i = 1, \dots, m) \tag{2}$$

Using $\mathbf{C}$ and the force density vector $\mathbf{q} \in \mathbb{R}^m$, the force density matrix $\mathbf{Q} \in \mathbb{R}^{m\times m}$ can be defined as

$$\mathbf{Q} = \mathbf{C}^T \mathrm{diag}(\mathbf{q})\mathbf{C} \tag{3}$$

The same matrix $\mathbf{Q}$ is used for obtaining the components of the nodal coordinates in x-, y-, and z-directions for specified force densities, because the ratios of axial force to length are all the same. The components are decomposed and re-ordered such that the components of free coordinates precede those of fixed nodes to re-assemble $\widetilde{\mathbf{Q}} \in \mathbb{R}^{3m\times 3m}$ as

$$\widetilde{\mathbf{Q}} = \left[\begin{array}{ccc|ccc} \mathbf{Q}^x_{\mathrm{free}} & \mathbf{0} & \mathbf{0} & \mathbf{Q}^x_{\mathrm{link}} & \mathbf{0} & \mathbf{0} \\ \mathbf{0} & \mathbf{Q}^y_{\mathrm{free}} & \mathbf{0} & \mathbf{0} & \mathbf{Q}^y_{\mathrm{link}} & \mathbf{0} \\ \mathbf{0} & \mathbf{0} & \mathbf{Q}^z_{\mathrm{free}} & \mathbf{0} & \mathbf{0} & \mathbf{Q}^z_{\mathrm{link}} \\ \hline \mathbf{Q}^{xT}_{\mathrm{link}} & \mathbf{0} & \mathbf{0} & \mathbf{Q}^x_{\mathrm{fix}} & \mathbf{0} & \mathbf{0} \\ \mathbf{0} & \mathbf{Q}^{yT}_{\mathrm{link}} & \mathbf{0} & \mathbf{0} & \mathbf{Q}^y_{\mathrm{fix}} & \mathbf{0} \\ \mathbf{0} & \mathbf{0} & \mathbf{Q}^{zT}_{\mathrm{link}} & \mathbf{0} & \mathbf{0} & \mathbf{Q}^z_{\mathit{fix}} \end{array}\right] = \left[\begin{array}{c|c} \widetilde{\mathbf{Q}}_{\mathrm{free}} & \widetilde{\mathbf{Q}}_{\mathrm{link}} \\ \hline \widetilde{\mathbf{Q}}^T_{\mathit{link}} & \widetilde{\mathbf{Q}}_{\mathrm{fix}} \end{array}\right] \tag{4}$$

where not only nodal coordinates at supported nodes but also those at loaded nodes are treated as fixed, since loaded nodes cannot move in geometry optimization of truss. Let n_{free} and n_{fix} denote the numbers of free and fixed coordinates, then the matrices $(\mathbf{Q}^x_{\mathrm{free}}, \mathbf{Q}^y_{\mathrm{free}}, \mathbf{Q}^z_{\mathrm{free}})$, $(\mathbf{Q}^x_{\mathrm{link}}, \mathbf{Q}^y_{\mathrm{link}}, \mathbf{Q}^z_{\mathrm{link}})$, $(\mathbf{Q}^x_{\mathrm{fix}}, \mathbf{Q}^y_{\mathrm{fix}}, \mathbf{Q}^z_{\mathrm{fix}})$ are combined to $\widetilde{\mathbf{Q}}_{\mathrm{free}} \in \mathbb{R}^{n_{\mathrm{free}}\times n_{\mathrm{free}}}$, $\widetilde{\mathbf{Q}}_{\mathrm{link}} \in \mathbb{R}^{n_{\mathrm{free}}\times n_{\mathrm{fix}}}$, $\widetilde{\mathbf{Q}}_{\mathrm{fix}} \in \mathbb{R}^{n_{\mathrm{fix}}\times n_{\mathrm{fix}}}$, respectively.

If the force densities of all members and fixed nodal coordinates $\mathbf{X}_{\text{fix}} \in \mathbb{R}^{n_{\text{fix}}}$ are specified, then the free nodal coordinates $\mathbf{X}_{\text{free}} \in \mathbb{R}^{n_{\text{free}}}$ are obtained from the following system of linear equations:

$$\widetilde{\mathbf{Q}}_{\text{free}}\mathbf{X}_{\text{free}} = -\widetilde{\mathbf{Q}}_{\text{link}}\mathbf{X}_{\text{fix}} \tag{5}$$

Therefore, $\mathbf{X}_{\text{free}}$ is a function of $\boldsymbol{q}$.

3. Optimization problem

3.1. Objective and constraint functions

Consider a problem for minimizing compliance under constraint on total structural volume.

The square of length L_i for member *i* that connects nodes *j* and *k* is given as

$$L_i^2 = \left(\mathbf{X}_{\text{k}} - \mathbf{X}_{\text{j}}\right)^T \left(\mathbf{X}_{\text{k}} - \mathbf{X}_{\text{j}}\right) \tag{6}$$

where $\mathbf{X}_{\text{j}} \in \mathbb{R}^3$ and $\mathbf{X}_{\text{k}} \in \mathbb{R}^3$ are the position vectors of nodes *j* and *k*, respectively.

It is known that the optimal solution to this problem is a statically determinate truss, and all the members have the same absolute value of stress $\overline{\sigma}$ (Hemp [10], Achtziger [4]). Hence, cross-sectional area of member *i* is expressed as

$$\begin{aligned} A_i &= \frac{|N_i|}{\overline{\sigma}} \\ &= \frac{|q_i|L_i}{\overline{\sigma}} \end{aligned} \tag{7}$$

Accordingly, total structural volume is expressed as

$$\text{V} = \sum_{i=1}^{m} \frac{|q_i|L_i^2}{\overline{\sigma}} \tag{8}$$

Strain energy S_i of member *i* is written using (8) as

$$\begin{aligned} S_i &= \frac{A_i L_i \overline{\sigma}^2}{2E} \\ &= \frac{\overline{\sigma}|q_i|L_i^2}{2E} \end{aligned} \tag{9}$$

Therefore, the compliance *F* is obtained as

$$\begin{aligned} F &= 2\sum_{i=1}^{m} S_i \\ &= \sum_{i=1}^{m} \frac{\overline{\sigma}|q_i|L_i^2}{E} \end{aligned} \tag{10}$$

3.2. Optimization problem

Equation (8) implies that $\overline{\sigma}$ is a scaling parameter for A_i of a statically determinate truss, for which N_i is independent of A_i. From (9) and (11), the product of *V* and *F* is computed as

$$\begin{aligned} VF &= \sum_{i=1}^{m} \frac{q_i^2 L_i^4}{E} \\ &= \sum_{i=1}^{m} \frac{N_i^2 L_i^2}{E} \end{aligned} \tag{11}$$

This means that VF is independent of $\bar{\sigma}$. Hence, the total structural volume can be calculated after minimizing the compliance with arbitrtary positive value $\bar{\sigma}$.

Define $\mathbf{R} \in \mathbb{R}^{n_{\text{fix}}}$ as the vector of reaction forces corresponding to $\mathbf{X}_{\text{fix}}$, which is obtained from

$$\mathbf{R} = \widetilde{\mathbf{Q}}_{\text{link}}^{T}\mathbf{X}_{\text{free}} + \widetilde{\mathbf{Q}}_{\text{fix}}\mathbf{X}_{\text{fix}} \tag{12}$$

As mentioned above, the locations of loaded nodes are fixed during the optimization. We treat loaded nodes as pin-supported and their reaction forces are prescribed in the optimization problem such that they are equalalent to the loading condition. Thus, the optimization problem can be formulated as

$$\begin{aligned} \text{minimize} \quad & F(\boldsymbol{q}) = \sum_{i=1}^{m} \frac{\bar{\sigma}|q_i|L_i^2}{E} \\ \text{subject to} \quad & R_i(\boldsymbol{q}) = \bar{R}_i \ \ (i \in \mathcal{R}) \\ & q_i^L \le q_i \le q_i^U \ \ (i \in 1, \dots, m) \end{aligned} \tag{13}$$

where $\mathcal{R}$ is a set of indices of reaction forces to be specified, and q_i^L and q_i^U are the lower and upper bound for q_i, respectively. Note that the design variables of this problem is the force densities only.

3.3. Improvement of convergence

We use sequential quadratic programming (SQP) that is categolized as a gradient-based nonlinear progaramming algorithm. Therefore, discontinuity in the function value and/or the sensitivity coefficient leads to serieious difficulty in convergence. So we use smoothing approximation for $|q_i|$ to avoid the nondifferentiability at $q_i = 0$ as

$$|q_i| = \sqrt{q_i^2 + c} \tag{14}$$

where *c* is a sufficiently small positive number.

Furthermore, we combine the constraint functions for R_i by using square norm as

$$\textstyle\sum_{i\in\mathcal{R}}(R_i(\boldsymbol{q}) - \bar{R}_\iota)^2 \le 0 \tag{15}$$

Note that we introduced an inequality expression in Eq. (15), because equality constraints are difficult to deal with in SQP. Therefore, the optimization problem (13) is reformulated in the following form:

$$\begin{aligned} \text{minimize} \quad & \tilde{F}(\boldsymbol{q}) = \sum_{i=1}^{m} \frac{\bar{\sigma}L_i^2\sqrt{q_i^2 + c}}{E} \\ \text{subject to} \quad & \textstyle\sum_{i\in\mathcal{R}}(R_i(\boldsymbol{q}) - \bar{R}_\iota)^2 \le 0 \\ & q_i^L \le q_i \le q_i^U \ \ (i \in 1, \dots, \mathrm{m}) \end{aligned} \tag{16}$$

3.4. Sensitivity analysis

To reduce the computation time for SQP, sensitivity coefficients of objective and constraint functions are necessary. Differentiation of (15) with respect to q_l is expressed in the form:

$$\frac{\partial\tilde{F}(\mathbf{q})}{\partial q_l} = \frac{\bar{\sigma}q_l L_l^2}{E\sqrt{q_l^2 + c}} + \textstyle\sum_{k=1}^{m}\left(\frac{\bar{\sigma}L_i^2\sqrt{q_i^2+c}}{E} \cdot \frac{\partial L_i^2}{\partial q_l}\right) \tag{17}$$

From (6), sensitivity coefficient of L_i^2 with respect to q_l is

$$\frac{\partial L_i^2}{\partial q_l} = 2\left(\mathbf{X}_\mathrm{k} - \mathbf{X}_\mathrm{j}\right) \cdot \frac{\partial\left(\mathbf{X}_\mathrm{k} - \mathbf{X}_\mathrm{j}\right)}{\partial q_l} \tag{18}$$

Differentiation of (5) with regard to q_l leads to

$$\widetilde{\mathbf{Q}}_\mathrm{free} \frac{\partial \mathbf{X}_\mathrm{free}}{\partial q_l} + \frac{\partial \widetilde{\mathbf{Q}}_\mathrm{free}}{\partial q_l} \mathbf{X}_\mathrm{free} = -\frac{\partial \widetilde{\mathbf{Q}}_\mathrm{link}}{\partial q_l} \mathbf{X}_\mathrm{fix} \tag{19}$$

Eq. (18) can be rearranged to obtain

$$\frac{\partial \mathbf{X}_\mathrm{free}}{\partial q_l} = -\widetilde{\mathbf{Q}}_\mathrm{free}^{-\mathbf{1}} \left(\frac{\partial \widetilde{\mathbf{Q}}_\mathrm{free}}{\partial q_l} \mathbf{X}_\mathrm{free} + \frac{\partial \widetilde{\mathbf{Q}}_\mathrm{link}}{\partial q_l} \mathbf{X}_\mathrm{fix}\right) \tag{20}$$

Besides, sensitivity coefficient of $(R_i - \bar{R}_l)^2$ with respect to q_l is derived as

$$\frac{\partial (R_i - \bar{R}_l)^2}{\partial q_l} = 2(R_i - \bar{R}_l) \cdot \frac{\partial R_i}{\partial q_l} \tag{21}$$

Sensitivity coefficients of reaction forces with respect to q_l are obtained by differentiating (7) as

$$\frac{\partial \mathbf{R}}{\partial q_l} = \frac{\partial \widetilde{\mathbf{Q}}_\mathrm{link}^T}{\partial q_l} \mathbf{X}_\mathrm{free} + \widetilde{\mathbf{Q}}_\mathrm{link}^T \frac{\partial \mathbf{X}_\mathrm{free}}{\partial q_l} + \frac{\partial \widetilde{\mathbf{Q}}_\mathrm{fix}}{\partial q_l} \mathbf{X}_\mathrm{fix} \tag{22}$$

Eq. (20) is incorporated into (18) and (22), which are further incorporated into (17) and (21), respectively, to successively obtain sensitivity coefficients of the objective and constraint functions with respect to force density.

3.5. Improvement of optimal solution

Since the optimal solution to Problem (16) may include overlapped nodes and members, and the nodal positions are obscure, we further optimize the cross-sectional areas and nodal coordinates for the solution. The re-optimization problem is formulated with fixed topology as

$$\begin{aligned} \text{minimize} \quad & F(\boldsymbol{X}, \boldsymbol{A}) = \sum_{i=1}^{m^*} \frac{N_i^2 L_i}{E A_i} \\ \text{subject to} \quad & \textstyle\sum_{i=1}^{m^*} A_i L_i \le \bar{V} \\ & X_i^L \le X_i \le X_i^U \quad (i \in 1, \dots, \mathrm{n}_\mathrm{free}^*) \\ & A_i^L \le A_i \le A_i^U \quad (i \in 1, \dots, m^*) \end{aligned} \tag{23}$$

where m^* and $\mathrm{n}_\mathrm{free}^*$ are the numbers of members and nodes after unifying the overlapped nodes and members. The lower bound A_i^L is a sufficiently small positive value, and the upper bound A_i^L is sufficiently large. The member with $A_i \cong A_i^L$ is eliminated after optimization.To avoid drastic change of an optimal shape, X_i^L and X_i^U are close to the initial value of X_i which is assigned based on the optimal solution of Problem (16).

4. Numerical examples

In this section, we present three examples to demonstrate accuracy, efficiency, and applicability of the proposed optimization method. We use the sequential quadratic programming algorithm SLSQP (Kraft [11]) in the optimization library NLopt (Johnson [12]) to solve NLP problems. Units are omitted in the following examples, since they are not important in this research.

Young's modulus is 1.0 for comparison purpose to the results in Achtiger [4]. The values of c in (14) and $\bar{\sigma}$ are 1.0×10^{-6} and 1.0, respectively. The upper bound of total structural volume is 10.0, and accordingly, the compliance F is scaled to $F^* = \tilde{F}V/10.0$ after optimization. Let $\bar{\boldsymbol{q}} = (\bar{q}_1, \ldots, \bar{q}_m)^T$ denote the set of force densities of the initial ground structure with uniform cross-sectional areas 1.0. The lower and upper bounds are set as $q_i^L = \bar{q}_i - 1.0 \times 10^3$ and $q_i^U = \bar{q}_i + 1.0 \times 10^3$, respectively. The initial values of force density for optimization are randomly provided within the range $[\bar{q}_i - 10.0, \bar{q}_i + 10.0]$. We choose the best solution after obtaining 100 solutions for 100 different random seeds.

4.1. 3 × 2 planar truss

The initial ground structure is a 3×2 rectangular grid with 27 members and 12 nodes including supports as shown in Figure 1. Nodes 1, 2, and 3 are pin-supported and node 11 is subject to downward unit load. The maximum, median, minimum, average values, and standard deviation of F^* for 100 trials are listed in Table 1. Diverse nearly optimal solutions have been found through 100 trials.

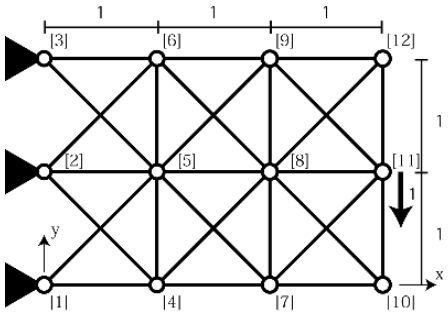

Figure 1: Initial ground structure of a 3×2 plane grid.

Table 1: Statistical results of values of F^* for 100 solutions

	3 × 2 planar truss	half-cone truss	5 × 5 spatial grid
max	37.659	150.491	10184.763
median	10.063	56.105	2064.496
min	8.404	43.419	1254.787
average	13.133	59.532	2401.357
std.dev.	6.425	14.193	1230.000

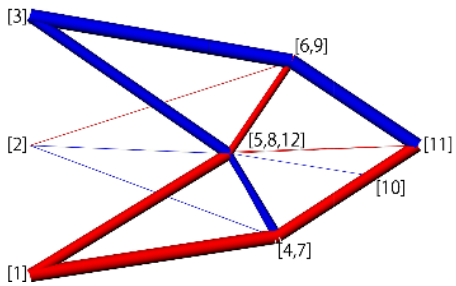

Figure 2: The best optimal solution ($F^* = 8.404$).

The best obtained solution to Problem (13) is shown in Figure 2. Red members are compressive and blue are tensile. The objective value $F^* = 8.404$ is almost equal to $F^* = 8.307$ obtained by Achtiger [4]. Although sets of nodes {5, 8, 12}, {4, 7}, and {6,9} are coalescent, no numerical error was observed.

In Figure 3, the histories of F^* for our proposed method is described. Note that the number of function call is not the number of major iterations of SQP, which involves minor iteration for solving QP subproblem and line search. Since nodal locations and cross-sectional areas of the members are indirectly controled by force densities, and no bounds are given for them, F^* widely fluctuates in the early stage of the optimization. However, this is irrelevant to the speed of satisfying optimality criteria; the number of objective function calls in this trial is 7515 until the optimizer stops. Actually, it takes 2.69 seconds for each trial on average, in which we use a PC with Intel Core i5 processor.

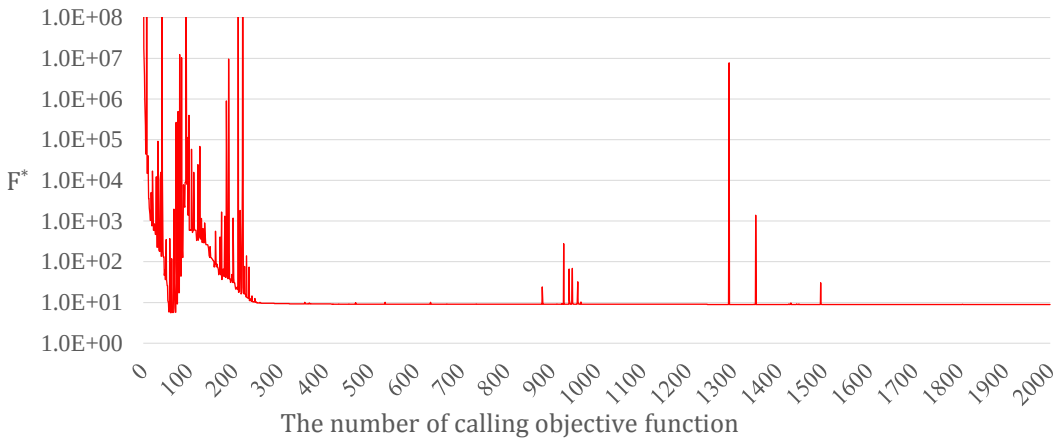

Figure 3: Iteration history of F^* of a typical trial of optimization.

Next, the solution in Figure 2 is post-processed solving Problem (23). The coalscent nodes are combined to one node, and node 10 and three thin members are removed before re-optimization. Hence, the model for the re-optimization has 6 nodes and 8 members. The optimal solution is shown in Figure 4, which is almost the same as the solution in Figure 2. The compliance F^* is slightly reduced to 8.341. Therefore, influence of post-processing is trivial and the proposed method leads to a sufficiently converged solution.

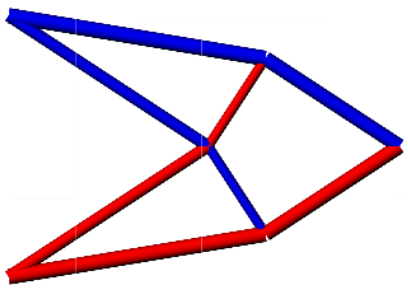

Figure 4: Solution of re-optimization for the result of Figure 2 ($F^* = 8.341$).

4.2. Half-cone truss

Consider a 30-bar half-cone truss, which is constructed by projecting congruent 16 isosceles triangles to the side of a cone as shown in Figure 5. Nodes 1, 11, and 15 are pin-supported and nodes 12, 13, and 14 are subjected to downward unit loads. As seen from Table 1, all the 100 solutions are converged.

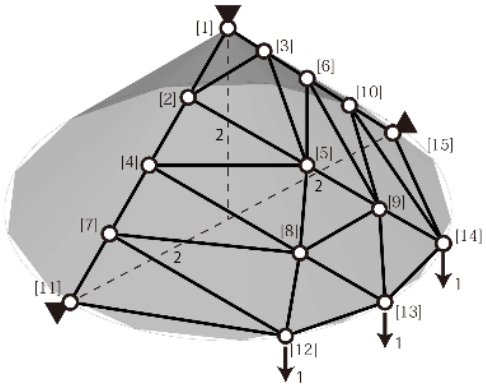

Figure 5: Initial ground structure of a half-cone truss.

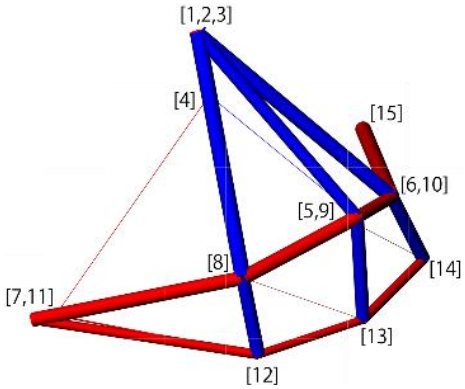

Figure 6: The best optimal solution ($F^* = 43.419$).

The best optimal solution obtained from 100 different random seeds is shown in Figure 6. The optimal shape is almost symmetric and includes sets of coalescent nodes {1, 2, 3}, {5, 9}, {6, 10} and {7, 11}. It takes only 17.45 seconds for each optimization.

4.3. 5 × 5 spatial grid

The last example is a 5 × 5 grid structure with 110 members. The initial ground structure as shown in Figure 7 is generated from four vertices (0,0,0), (5,0,0), (0,5,0), (5,5,5) using a Grasshopper Lunchbox component, which is a designer-friendly geometry generation tool. The vertices are pin-supported and all the other points on the edges are subjected to downward unit loads. From the maximum value of F^* for 100 trials in Table 1, it is confirmed that all the optimization results are converged.

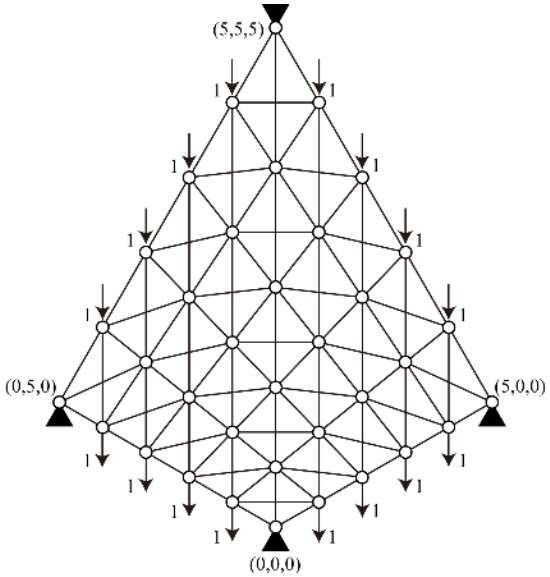

Figure 7: Initial ground structure of a 5×5 grid truss.

The best optimal solution is shown in Figure 8. Symmetry can be seen in the optimal shape. It takes 1673.82 seconds for the iteration.

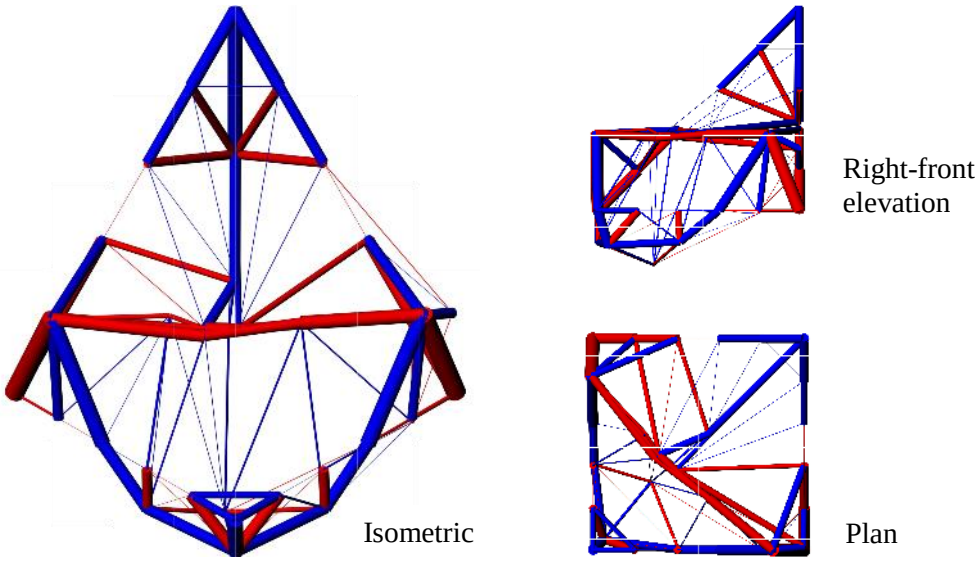

Figure 8: The best optimal solution ($F^* = 1254.787$).

5. Conclusion

The difficulty in simultaneous optimization of geometry and topology due to melting nodes can be successfully avoided using force density as design variable, which allows to obtain a variety of solutions of geometry and topology. Moreover, absolute values of force density are smoothed and multiple constraint functions are integrated by using a sum of square norms in the formulation. Applicability and accuracy of the proposed method have been verified through numerical examples of both plane and

spatial trusses. Furthermore, the number of design variables can be reduced to the number of members. By combining this benefit and sensitivity analysis, computational cost has been drastically reduced.

Acknowledgements

This work is partially supported by JSPS KAKENHI No.16H03014 and "The John Mung Program for Students" of Kyoto University.

References

[1] M. P. Bendsøe and O. Sigmond, Topology Optimization: Theory, Methods and Applications, Springer, 2003.

[2] M. Ohsaki, Simultaneous optimization of topology and geometry of a regular plane truss, Comput. & Struct., Vol. 66(1), pp. 69–77, 1998.

[3] W. R. Dorn, R. Gomory and H. Greenberg. Automatic design of optimal structures, J. de Mecanique; Vol. 3: 25–52, 1964.

[4] W. Achtziger, On simultaneous optimization of truss geometry and topology, Struct. Multidisc. Optimiz., Vol. 33, pp. 285–304, 2007.

[5] J. J. McKeown, Growing optimal pin-jointed frames, Struct. Opt., Vol. 15, pp. 92–100, 1998.

[6] T. Hagishita and M. Ohsaki, Topology optimization of trusses by growing ground structure approach, Struct. Multidisc. Optim., Vol. 37(4), pp. 377–393, 2009.

[7] M. Ohsaki and K. Hayashi, Force density method for simultaneous optimization of geometry and topology of trusses, submitted to Struct. Multidisc. Optim.

[8] H.-J. Schek. The force density method for form finding and computation of general networks, Comput. Methods Appl. Mech. Eng.; Vol. 3: pp. 115–134, 1974.

[9] J. Y. Zhang and M. Ohsaki. Tensegrity Structures. Form, Stability, and Symmetry. Mathematics for Industry 6. Springer, 2015.

[10] W. S. Hemp, Optimum Structures, Clarendon Press, Oxford, UK, 1973.

[11] D. Kraft, A software package for sequential quadratic programming, Technical Report DFVLR-FB 88-28, 1988.

[12] S. G. Johnson, The NLopt nonlinear-optimization package, http://ab-initio.mit.edu/nlopt